Experimental Evidence of Stress-Induced Critical State in Schooling Fish

Guozheng Lin,[1,2,3] Ramón Escobedo,[1] Xu Li,[1,4] Tingting Xue,[1,4] Zhangang Han,[2] Clément Sire,[5] Vishwesha Guttal,[6] and Guy Theraulaz[1,*]

[1]*Centre de Recherches sur la Cognition Animale, Centre de Biologie Intégrative, CNRS, Université de Toulouse III–Paul Sabatier, 31062 Toulouse, France*

[2]*School of Systems Science, Beijing Normal University, Beijing 100875, China*

[3]*School of Systems Science, Beijing Jiaotong University, Beijing 100091, China*

[4]*Faculty of Science, Kunming University of Science and Technology, Kunming 650500, China*

[5]*Laboratoire de Physique Théorique, CNRS, Université de Toulouse III–Paul Sabatier, 31062 Toulouse, France*

[6]*Center for Ecological Sciences, Indian Institute of Science, Bengaluru, India*

(Received 21 February 2025; accepted 8 August 2025; published 4 September 2025)

How animal groups dynamically adjust their collective behavior in response to environmental changes remains an open and challenging question. Here we investigate the mechanisms that allow fish schools to tune their collective state under stress, testing the hypothesis that these systems operate near criticality, a state that maximizes sensitivity, responsiveness, and adaptability. We combine experiments and data-driven computational modeling to study how group size and stress influence the collective behavior of rummy-nose tetras (*Hemigrammus rhodostomus*). We quantify the collective state of fish schools using polarization, milling, and cohesion metrics and use a burst-and-coast model to infer the social interaction parameters that drive these behaviors. Our results indicate that group size modulates stress levels, with smaller groups experiencing higher baseline stress, likely due to a reduced social buffering effect. Under stress, fish adjust the strength of their social interactions in a way that leads the group into a critical state, thus enhancing its sensitivity to perturbations and facilitating rapid adaptation. However, while large groups require an external stressor to enter the critical regime, small groups are already near this state. Our findings suggest that adjusting interaction strength is a simple yet effective mechanism that drives collective state transitions while minimizing individual cognitive load. By revealing how stress and group size drive self-organization toward criticality, our study provides fundamental insights into the adaptability of collective biological systems and the emergent properties in animal groups.

DOI: 10.1103/nr7p-m4ff

I. INTRODUCTION

Collective behaviors in biological systems have intrigued scientists for decades [1,2]. These phenomena are observed at all scales of biological organization from macromolecules and cell constituents to groups of organisms, and they result from the ability of these biological entities to self-organize and coordinate their actions through their interactions [3–5]. A fundamental question is to understand the adaptive significance of collective behavior in contexts such as environmental changes or to escape dangers [6].

Recently, the concept of criticality derived from statistical mechanics [7] has emerged as a compelling lens through which one can understand the mechanisms underlying adaptability in biological systems. The criticality hypothesis suggests that biological systems should operate at or close to critical points or critical lines that demarcate qualitative changes in collective behaviors and organizations in the phase diagram of parameters, akin to phase transitions in physics [8]. When a biological system is in a critical state, it offers unique properties that maximize its sensitivity to external perturbations and enhance collective information processing and its adaptability in response to environmental cues [9–11].

Recent empirical evidence has begun to shed light on the relevance of criticality in various biological systems. From neural dynamics [12–15] to gene regulation, aggregation in social amoeba [16], and collective motion in animal groups [17,18], studies have reported instances of scale invariance and critical behavior. In particular, research on spontaneous behavioral cascades and escape waves in schooling fish has provided valuable insights into how these systems could operate near criticality [19,20].

Fish schools could also modulate the distance to criticality according to the environmental context. In groups of juvenile golden shiners (*Notemigonus crysoleucas*), it has been suggested that when the perceived risk increases, the distance to criticality decreases [21]. Thus, fish schools would be able to achieve a fine balance between their sensitivity and the robustness of their collective responses as a function of the riskiness

*Contact author: guy.theraulaz@univ-tlse3.fr

and noise of the environmental conditions. In that context, a crucial open question is that of the actual mechanisms used by these animal collectives to tune themselves toward the critical region of the parameter space [22].

Here we address this question through the study of collective phase changes in schooling fish in response to a stressing condition. We combine experiments with computational modeling to investigate how group size and stress affect the way fish swim and interact with each other, and the consequences on the collective behavior exhibited by groups of rummy-nose tetras (*Hemigrammus rhodostomus*). Our results suggest that the stress state of individuals is strongly modulated by group size, presumably due to a social buffering effect [23,24]. Moreover, when the fish are stressed, they spontaneously adjust the intensity of their social interactions such that the shoal collectively reaches the proximity of a critical state, which allows it to rapidly adapt its behavior in response to changes occurring in the environment.

II. RESULTS

Before addressing our experimental setup and the corresponding modeling, we wish to briefly describe the typical properties of fish school models, and in particular those of the data-driven behavioral model exploited here [25,26]. These active matter models generally include an attractive pairwise interaction between individuals (becoming repulsive at short range) and an alignment pairwise interaction. The collective state of the group is characterized by two *order parameters*, the polarization P, and the milling parameter M (see Materials and Methods). P quantifies the mean heading of the group and is similar to the magnetization of physical spin systems. High values of P characterize a schooling group of well-aligned individuals. M is similar to an angular momentum, and high values of M signal that the group is rotating around its center of mass. Finally, when both P and M are small, the group is in a swarming state with no particular orientational order. These three collective states are commonly observed in real fish schools [27]. As the intensity of both attraction and alignment interactions are varied/scanned, one can build the *phase diagram* of the model, resulting in transition/critical lines delimiting the schooling, milling, and swarming phases. Such phase diagrams have been obtained for data-driven fish school models built to describe the smooth swimming mode of fish such as *Kuhlia mugil* [28], including when taking into account hydrodynamic effects in open [29] or confined [30] space. For fish displaying a burst-and-coast swimming mode, such as rummy-nose tetra (*Hemigrammus rhodostomus*) or zebrafish (*Danio rerio*), where fish alternate sudden and short acceleration periods with longer gliding periods in a quasistraight line, similar phase diagrams have been obtained [31,32].

In practice, these phase diagrams are generated using finite groups (typically $N = 100$–200 agents in [28–32]), and the sharp transitions expected in the thermodynamic limit $N \to \infty$ are replaced by smooth crossovers. Accordingly, these transition lines between the different phases become sharper as N increases, separating ordered regions, where the relevant order parameter (P or M) weakly depends on N and remains nonzero as N increases, and regions where the corresponding order is lost, and the order parameter vanishes like $1/\sqrt{N}$.

Interestingly, it has been shown that such behavioral models qualitatively satisfy an equivalent of the fluctuation-dissipation theorem (FDT) in physics: the response of the group to a small perturbation (say, the change in the polarization due to a few agents with different interaction parameters than those of the main group) is proportional to the fluctuations present in the system (say, the variance of polarization) *without* any perturbation [9]. In particular, as the interaction parameters are varied to cross a critical line between two collective states, one observes that both the susceptibility characterizing the response to a perturbation and the fluctuations of the corresponding order parameter reach a maximum at the transition point. This divergence (strictly speaking, only in the $N \to \infty$ limit) of both the susceptibility and fluctuations is well understood in critical physical systems like spin systems, but has an interesting biological interpretation in the context of fish schools and, more generally, living groups: having its effective interaction parameters close to a transition line allows a living group to quickly react to a perturbation, in practice, a change in its environment, such as the presence of a predator, danger, or food.

In the present work, we aim at identifying the effective interaction parameters of groups of $N = 10$ and $N = 25$ rummy-nose tetra fish as they are subjected to a mild stress produced by a sudden change of light. In particular, we are interested in locating their collective state and effective interaction parameters in the phase diagram of a faithful data-driven model that has been shown to quantitatively reproduce their motion dynamics [25,26], including for different stationary light conditions [33].

A. Effect of mild stress on collective swimming behavior

The experiment consists of inducing mild stress in a group of fish by abruptly increasing the intensity of light from 0.5 lx to 25 lx. Each of our experiment begins with a 10-min habituation period at 0.5 lx. A sudden change in the light intensity is then repeated 10 times, involving a series of 2-min intervals at 0.5 lx alternating with 1 min intervals at 25 lx (see Fig. 1). This latter condition, called the *Stressing condition*, is replicated six times with groups of $N = 10$ and $N = 25$ fish (see Movies S1 and S2 in the Supplemental Material [34]). In the *Control condition*, the light intensity is kept to a constant value of 25 lx. Here, too, each experiment begins with a 10-min habituation period, and the fish behavior is then recorded for 1 h with no changes in light intensity. The Control condition is replicated four times with groups of $N = 10$ and $N = 25$ fish (see Movies S3 and S4 [34]). Details on the experimental protocol are provided in Sec. IV A.

Previous studies have shown that when fish are subjected to a sudden increase in light, their physiological response is very similar to that induced by a threat and resulted in a very high increase in oxygen consumption [35]. Here, as depicted in Figs. 1(a)–1(f), sudden changes in light conditions induce qualitative shifts in the collective motion of fish groups. We quantify collective motion via three group-level instantaneous observables: polarization $P(t)$, which measures the degree of alignment of fish; milling $M(t)$, which measures the collective rotation of the group around the center of the tank; and dispersion $D(t)$, which measures the spread of the group. The

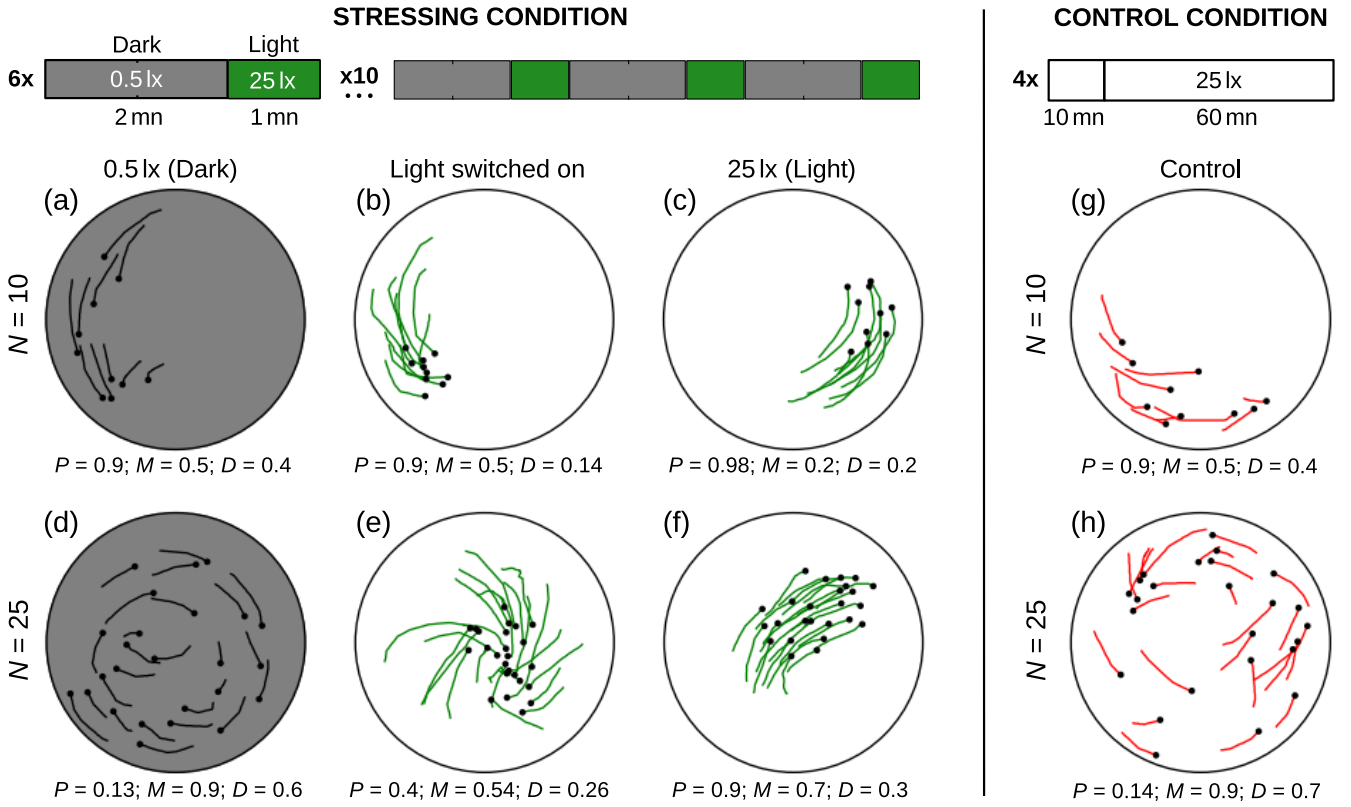

FIG. 1. Representative states of fish groups swimming in a circular tank of radius $R = 25$ cm in the Stressing and Control conditions. (a)–(f) Stressing condition: Six replicates of 10 periods of 3 min for each group size, alternating low light intensity (Dark, 0.5 lx during 2 min) and high light intensity (Light, 25 lx during 1 min). (a), (d) Snapshots of a group of $N = 10$ and $N = 25$ right before the increase in light intensity, (b), (e) right after, and (c), (f) 30 sec later. (g), (h) Control condition: Four replicates of 70 min at constant high light intensity (25 lx) for each group size. Snapshots of a group of $N = 10$ and $N = 25$ in the Control condition. Black dots represent fish positions, and the black, green, and red lines are the individual trajectories over the past 1 sec. The instantaneous values of polarization $P(t)$, milling $M(t)$, and dispersion $D(t)$ are provided for each spatial snapshot.

three observables take dimensionless values in [0,1], and their mathematical expressions are given in Sec. IV B.

When the intensity of light increases, the fish immediately move towards each other while remaining closer to each other, leading to a decrease in the dispersion $\langle D\rangle(t)$ from 0.42 at 0.5 lx to 0.22 in groups of 10 fish [Fig. 2(c)], and from 0.64 to 0.4 in groups of 25 fish [Fig. 2(f)]. Then, during the next 60 sec at 25 lx, the fish disperse slightly again, but still remain relatively more cohesive than at 0.5 lx or in the Control condition [red solid lines, Figs. 2(c) and 2(f)]. In both group sizes, the high cohesion, combined with the propensity to swim near the wall, gives rise to higher polarization [Figs. 2(a) and 2(d)] and smaller milling [Figs. 2(b) and 2(e)]. This effect is more pronounced in large groups: $\langle P\rangle(t)$ grows from 0.65 to 0.83 in small groups [Fig. 2(a)] and from 0.25 to 0.55 in large groups [Fig. 2(d)], while $\langle M\rangle(t)$ decreases from 0.53 to 0.40 in small groups [Fig. 2(b)] and from 0.73 to 0.49 in large groups [Fig. 2(e)].

Then, when the light intensity drops again, the fish disperse and recover in less than 30 sec to the state they initially were at in low light intensity. Figures 2(c) and 2(f) show that dispersion quickly recovers a constant "rest" value (exactly the control value when $N = 10$, and close to the control value when $N = 25$) with a relaxation time of about 10 sec in both group sizes. This contrasts with the dynamics observed after the increase in light intensity, in which the relaxation time of the dispersion is much longer in both group sizes (over 60 sec). Together, these results suggest that the increase in light intensity induces a change in the behavioral state of fish that is not simply due to higher cohesion of fish at 25 lx, but a consequence of the stress induced by the sudden change in the light condition.

To accurately compare the difference between the state of fish at 25 lx having experienced an abrupt change in light condition and the state of fish that have been exposed to a constant light intensity of 25 lx, we computed the probability density functions (PDF) of polarization, milling, and dispersion in the Stressing (black and green solid lines in Fig. 3) and Control (red solid lines in Fig. 3) conditions. With the exception of milling in small groups [Fig. 3(b)], the three measures exhibit clear differences between the Light period of the Stressing condition and the Control condition for both group sizes, while the values observed in the Dark period of the Stressing condition and in the Control condition are relatively similar.

Dispersion is smaller in the Light period of the Stressing condition than in the Control condition [Figs. 3(c) and 3(f)] for both groups. Polarization and milling, however, show some group size dependence. In small groups, the polarization is high with a mode at $P \approx 0.95$ [Fig. 3(a)], meaning that fish

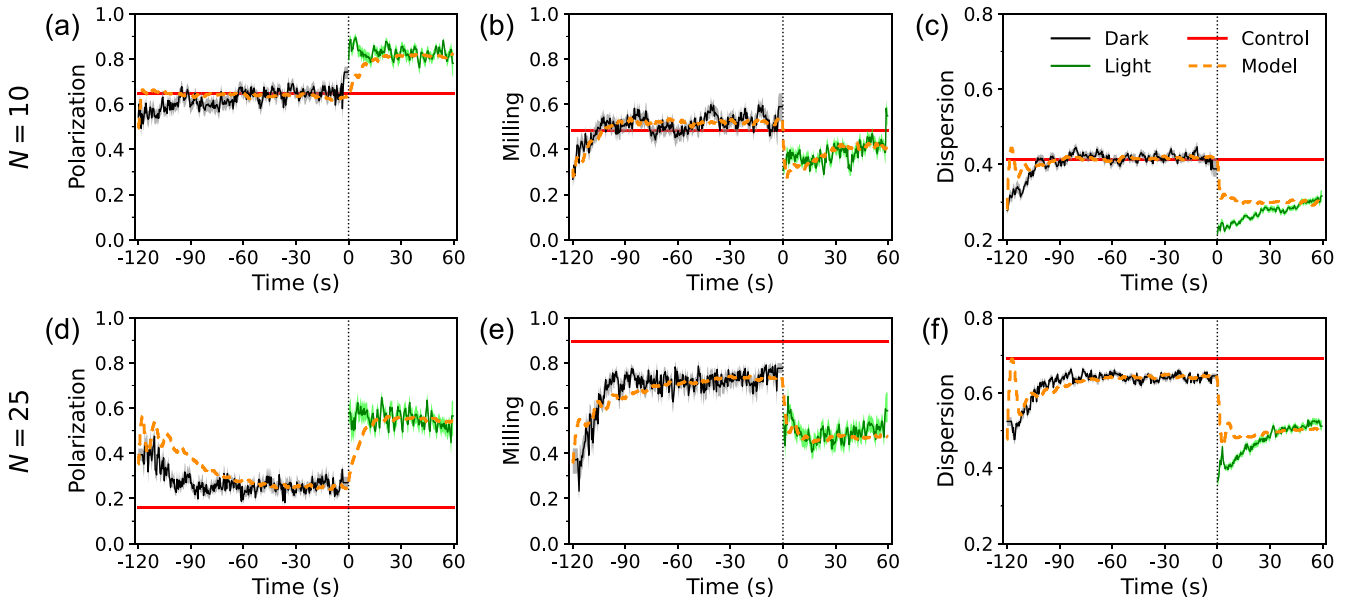

FIG. 2. Temporal dynamics of collective observables. Time series of polarization, milling, and dispersion, averaged over repeated conditions, in the Dark (black lines) and Light (green lines) periods of the Stressing condition, for $N = 10$ and $N = 25$ fish. Solid lines represent the experimental results, red lines the mean value of the Control condition, and orange dashed lines the numerical simulations of the model. The shaded areas represent the 68% confidence interval (bootstrap of 1000 rounds) for the experimental results. The vertical black dotted line indicates the time at which the light is switched on. Mean $\pm$ standard deviation from the last 30 sec of Dark condition to the last 30 sec of Light condition for $N = 10$: $P = 0.65 \pm 0.22$ to 0.83 ± 0.18, $M = 0.53 \pm 0.26$ to 0.40 ± 0.22, $D = 0.42 \pm 0.08$ to 0.28 ± 0.06. And for $N = 25$: $P = 0.25 \pm 0.16$ to 0.55 ± 0.24, $M = 0.73 \pm 0.19$ to 0.49 ± 0.25, $D = 0.64 \pm 0.04$ to 0.49 ± 0.07.

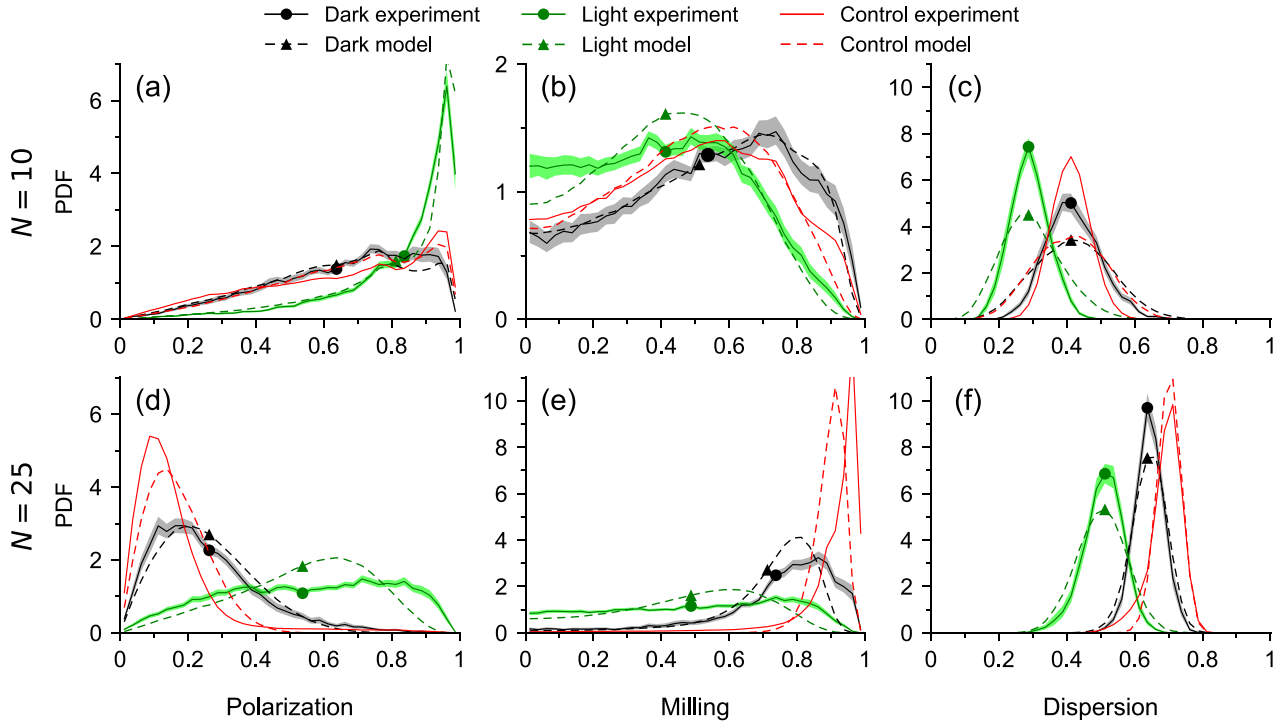

FIG. 3. Distributions of collective observables. Probability density function (PDF) of the polarization, milling, and dispersion observed in groups of $N = 10$ fish (a)–(c) and $N = 25$ fish (d)–(f) in the Stressing (dark and green solid lines) and Control (red solid lines) conditions, together with the results of the numerical simulations of the model (dashed lines). The shaded areas represent the 68% confidence interval (bootstrap of 1000 rounds) for the experimental results. Colored symbols represent mean values also reported in Table S2 [34].

are very often extremely well aligned, much more than what was suggested by the mean value in Fig. 3(a). The small bump visible at $P \approx 0.8$ in Fig. 3(a) corresponds to the situation where all the fish of the group except one are directionally aligned ($P \approx (9-1)/10 = 0.8$). In the Dark period of the Stressing condition [black solid line in Fig. 3(a)] and in the Control condition [red solid line in Fig. 3(a)], the PDF is more uniformly distributed, and where the small bump at $P \approx 0.8$ is still visible. In small groups, the PDF of the milling in the Light period of the Stressing condition is similar to the one observed in the Control or Dark period of the Stressing condition [Fig. 3(b)], contrary to what is observed with the polarization [Fig. 3(a)].

In large groups, the differences between the Light period of the Stressing condition and the Control condition are much more evident. In the Control condition, polarization is weak $\langle P \rangle = 0.16$ with a mode at $P \approx 0.1$ [see Table S2 [34] and red solid line in Fig. 3(d)], a value which is comparable to the mean polarization of $\langle P \rangle = \frac{1}{2}\sqrt{\pi/N} \approx 0.177$ expected assuming uncorrelated random orientations of fish. Milling is also quite high, with $\langle M \rangle = 0.90$ and peaked at $M \approx 0.95$ [see Table S2 [34] and red solid line in Fig. 3(e)]. Low polarization $\langle P \rangle = 0.25$ and high milling $\langle M \rangle = 0.73$ [see Table S2 [34] and black solid lines in Figs. 3(d) and 3(e)] are also observed in the Dark period of the Stressing condition. These PDFs together with the visual inspection of the videos show that in both the Control and in the Dark period of the Stressing conditions, the fish rotate along the edge of the tank, with the same direction of rotation leading to a high value of M and consequently, a small value of P. By contrast, in the Light period of the Stressing condition, the PDFs of polarization and milling are both almost uniform [green solid lines in Figs. 3(d) and 3(e)].

In the next section, we use a data-driven behavioral model to unveil the mechanisms by which groups of fish react to the Stressing condition and how these observed dynamics reflect the proximity to a critical region.

B. Modeling collective response of fish school to intermittent light condition

We use the burst-and-coast model introduced in [25] that describes the swimming mode and social interactions of *H. rhodostomus* also interacting with the wall of the circular tank. This model has been extended in [33] to account for the modulation of social interactions between fish and their reactions to obstacles by light intensity (ranging from 0.5 lx to 50 lx) and its impact on collective motion patterns in groups of different sizes, spanning the range $N = 1$ to 25. Our broad strategy is as follows: We first parametrize the values of movement and social interactions that shape the collective movement of fish schools in Control, Dark, and Light conditions. We then construct the phase diagram of the model and ask if the estimated parameters lie in the vicinity of transitions between different collective motion phases.

The model is based on the assumption that the behavior of a fish results from the combination of three factors: the spontaneous behavior of fish characterized by stochastic spontaneous heading changes of amplitude γ_R; the repulsion of the wall of the tank, of intensity γ_w; and the effect of social interactions, consisting of long-range attraction/short-range repulsion and alignment interactions, whose strength is denoted γ_{Att} and γ_{Ali}, respectively. Moreover, based on previous empirical evidence, the model considers that at each time each fish only interacts with its two most influential neighbors and combines their influence in an additive form (see Sec. IV C for a detailed description of the model). The model simulates the behavior of N fish under each light condition and provides the individual trajectory of each fish.

TABLE I. Estimation of parameter values of the noise (γ_R), the strength of attraction (γ_{Att}), and the strength of alignment (γ_{Ali}) in the Control and Stressing conditions (Dark and Light periods) and for each group size. In the Dark and Light periods, the values have been estimated 30 sec after the change of light intensity. In the Stressing condition, arrows indicate the variation of the parameter values after the change of light intensity.

	$N = 10$				$N = 25$			
	Control	Dark		Light	Control	Dark		Light
γ_R	0.24	0.2	↘	0.04	0.04	0.16	↗	0.34
γ_{Att}	0.023	0.026	↗	0.034	0.013	0.018	→	0.016
γ_{Ali}	0.022	0.023	→	0.025	0.004	0.007	↗	0.021

The numerical simulations carried out in [33] show that fish adapt their swimming behavior and social interactions to each light condition ranging from 0.5 lx to 25 lx, and for different group sizes spanning from $N = 1$ to 25, essentially through the modulation of the three parameters γ_R, γ_{Att}, and γ_{Ali}, while the other parameters remain unchanged. We therefore explore the 3D parameter space of $(\gamma_R, \gamma_{Att}, \gamma_{Ali})$ to find the values for which the model best reproduces the experimental results obtained in the three lighting conditions. We have kept the parameter values that remain unchanged equal to those determined in [33]. The result is a triplet of values $\boldsymbol{\gamma} = (\gamma_R, \gamma_{Att}, \gamma_{Ali})$ for each light condition and each group size (see Table I). The procedure used to determine the parameter values in the three lighting conditions is described in detail in Sec. IV D.

In the Stressing condition, the sudden increase in light intensity leads to a change in the strength of interactions between fish. However, this effect also depends on the size of the group. In groups of $N = 10$, fish react by increasing the attraction strength, while in groups of $N = 25$, fish increase the alignment strength. At the same time, the spontaneous heading changes of fish γ_R decrease in groups of $N = 10$ fish, but increase in groups of $N = 25$ fish. These results suggest that the impact of stress on fish depends on the size of the group. With the exception of γ_R in groups of $N = 25$ fish, the parameter values between the Control and the Dark conditions are comparable. In both group sizes, the intensity of social interactions is similar, but the amplitude of the spontaneous heading changes of fish is much smaller in the Control condition than in the Dark in groups of $N = 25$ fish.

During the fitting procedure of data under the Stressing condition, we observed that the time evolution of the parameters γ_{Att} and γ_{Ali} in response to abrupt changes in light could not be accurately modeled using a simple step function. In particular, the transitions observed in Fig. 2 display

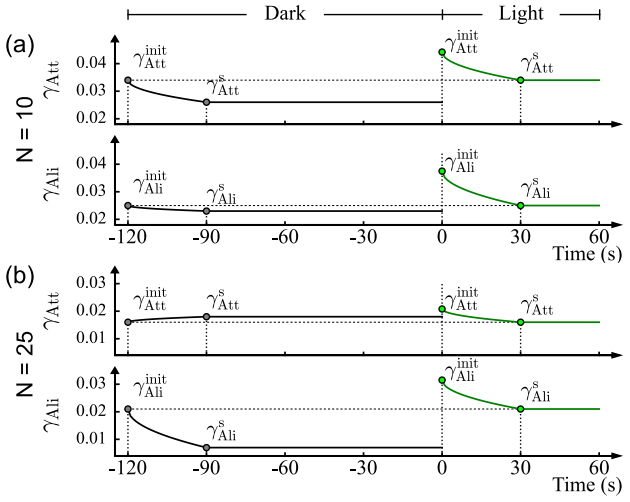

FIG. 4. Time profiles of the strengths of attraction γ_{Att} and alignment γ_{Ali} interactions used in the numerical simulations for (a) $N = 10$ and (b) $N = 25$. After each increase or decrease in light, the intensities of γ_{Att} and γ_{Ali} vary from their initial values during a habituation period of 30 sec and then keep a constant value. The initial parameter values in the Dark period are exactly the same as those at the end of the previous Light period. When the light is switched on, the attraction and alignment strengths are assumed to take initial values $\gamma_{\mathrm{Att}}^{\mathrm{init}}$ and $\gamma_{\mathrm{Ali}}^{\mathrm{init}}$ and then decrease to reach their stationary value, $\gamma_{\mathrm{Att}}^{\mathrm{s}}$ and $\gamma_{\mathrm{Ali}}^{\mathrm{s}}$, over a period of 30 sec. In the following, references to parameter values under a given condition correspond to their stationary (i.e., time-asymptotic) values indicated by the white crosses in Figs. 5 and 6.

distinct temporal asymmetries: a sharp, immediate increase when switching from Dark to Light, and a slower, progressive decrease when returning from Light to Dark. To account for this asymmetry, we introduced a 30-sec *habituation phase* at the beginning of each lighting period, as illustrated in Fig. 4. Specifically, when the system enters the Light condition, γ_{Att} and γ_{Ali} instantaneously jump to high transient values—reflecting an acute response to the light stimulus, and then decay smoothly towards their Light-period steady—state values over 30 sec. Conversely, upon switching to the Dark condition, the parameters retain their previous Light-period values for a short interval and then gradually transition to the Dark-period steady-state values, also over a 30-sec timescale. This temporal modeling captures the observed lag in behavioral adjustment and reflects the process of sensory adaptation in fish schools exposed to light stress. A complete mathematical description of the transition functions and their parametrization is provided in Sec. IV D.

Figures 2 and 3 reveal a good agreement between the experimental (solid lines) and simulation results (dotted lines) for all three conditions, including in the moments that immediately follow the changes in light intensity, when the fast collective response of fish to environmental changes is challenging to reproduce (see also Movies S5–S8 [34]). In particular, the model reproduces the PDF of polarization, milling, and dispersion for all lighting conditions and for both group sizes. Figures 8 and 9 also show that the model reproduces the distance of fish to the wall $\langle r_{\mathrm{w}}\rangle/R$ and the distance of fish to the nearest neighbor (NND) observed in the experiments.

In the Stressing condition, the agreement is excellent in the 60 sec before the light is turned on and, in most cases, even during the 2 min at 0.5 lx, as shown in Fig. 2. This is also the case during the 30 sec following the transition time, i.e., in the last 30 sec during which the light is at 25 lx. During the interval immediately following the light changes, the model takes some time to adapt to the new light intensity (a short delay of 10 to 20 sec depending on the observable) to adjust to the experimental value. Overall, the model reproduces the transient regime for the polarization and the milling order parameters [Figs. 2(a), 2(b), 2(d), and 2(e)], but fails to capture this regime for the dispersion. A possible interpretation is that this transient regime may also be controlled by variations in the speed of the fish (not included in the model), which would affect the dispersion more than the polarization and milling order parameters (which depend solely on headings but not on the magnitude of the individual velocities).

Together, these results suggest that the modulation of the collective behavior of fish in the Stressing condition results from the variation of amplitude of the spontaneous heading change of fish and the strength of the social interactions between fish.

C. Impact of a mild stress on social interactions and phase diagram

The behavior of a dynamical system near phase transitions and the definition of critical states are better established in systems with a large number of particles, ideally in the infinite size limit. Although we are working with quite small systems, via the agent-based model, we demonstrate that our fish shoals tune towards critical points.

Figures 5 and 6 show the phase diagrams for the polarization and milling order parameters, and the dispersion, in the Dark and Light periods of the Stressing condition, and in the Control condition, for each group size. They are represented in the γ_{Att}-γ_{Ali} plane, together with the diagrams of fluctuations of each quantity, $\mathcal{X}_P$ and $\mathcal{X}_M$ (in physics, linked to susceptibilities by the fluctuation-dissipation theorem), measured by the variance of the corresponding order parameter times the group size. The value of γ_{R} is also indicated for each condition. In each diagram, the value $(\gamma_{\mathrm{Att}}^{*}, \gamma_{\mathrm{Ali}}^{*})$ that better reproduces the experimental results in our simulations is represented by a *white cross* symbol. The location of the maxima of the variance/fluctuations of the polarization and milling order parameters has been determined along vertical and horizontal cuts/scans of the phase diagrams, selecting the appropriate search direction in multivalued cases. These critical lines estimated from the fluctuations of the order parameters are indeed consistent with and delimitating the regions where the order parameters take a significant value (red and blue regions for the polarization and milling parameters). Let us first consider the case of $N = 25$ fish (see also Fig. S3 [34], where P and M are plotted along 1D cross sections of the phase diagram). Figures 5(a) and 5(g) show that in the Dark period of the Stressing condition, the system is in a state where the polarization is low ($P < 0.3$) and the milling is relatively high ($M > 0.7$). What is important here is not the absolute

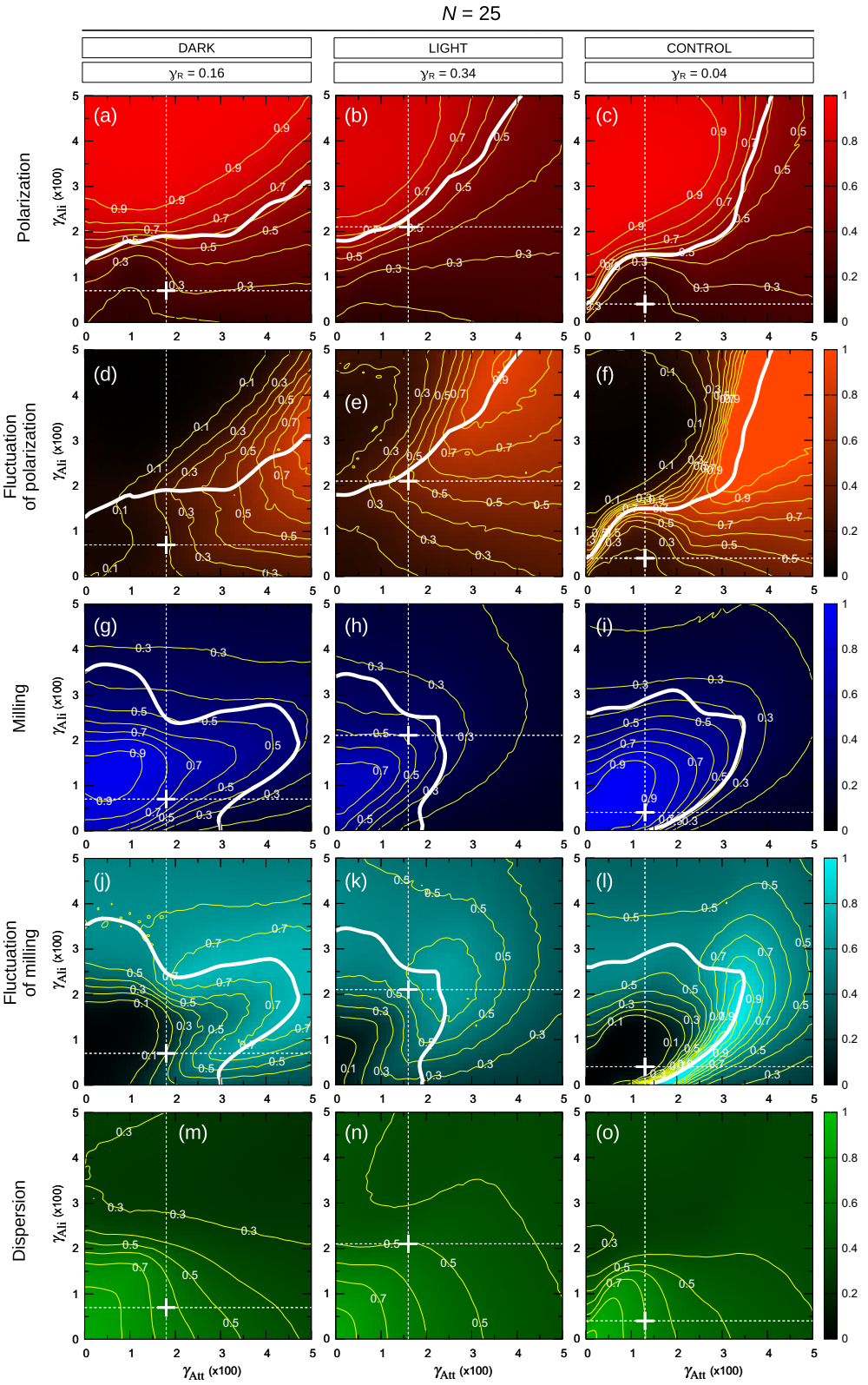

FIG. 5. Polarization (a)–(c), fluctuations of polarization (d)–(f), milling (g)–(i), fluctuations of milling (j)–(l), and dispersion (m)–(o) as functions of the intensity of attraction γ_{Att} and alignment γ_{Ali}, for the Dark (left) and Light (middle) periods of the Stressing condition and the Control condition (right) in groups of $N = 25$ fish. Fish interact with their two most influential neighbors. We also show the critical lines estimated from the local maxima of the fluctuations of the corresponding order parameters (thick white line). The white cross and dashed white lines indicate the stationary value of $(\gamma^*_{\mathrm{Att}}, \gamma^*_{\mathrm{Ali}})$ that best reproduces the experimental results in the numerical simulations. The value of the noise γ_{R} for each condition is also shown. The estimated interaction parameters are far from the critical region for the Dark and Control conditions, and lie in this region is the Light condition.

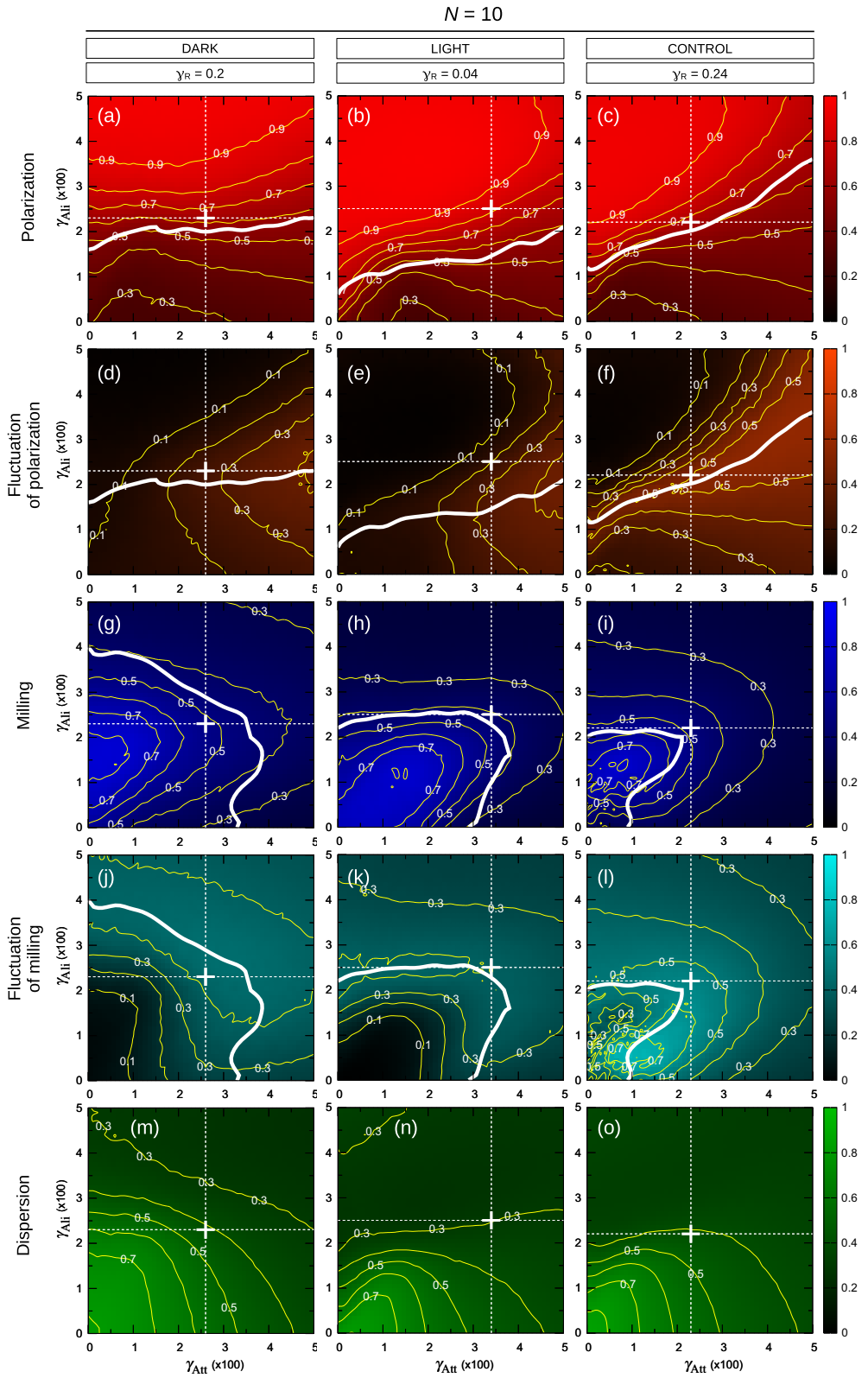

FIG. 6. Polarization (a)–(c), fluctuations of polarization (d)–(f), milling (g)–(i), fluctuations of milling (j)–(l), and dispersion (m)–(o) as functions of the intensity of attraction γ_{Att} and alignment γ_{Ali}, for the Dark (left) and Light (middle) periods of the Stressing condition and the Control condition (right) in groups of $N = 10$ fish. Fish interact with their two most influential neighbors. We also show the critical lines estimated from the local maxima of the fluctuations of the corresponding order parameters (thick white line). The white cross and dashed white lines indicate the stationary value of $(\gamma^*_{\mathrm{Att}}, \gamma^*_{\mathrm{Ali}})$ that best reproduces the experimental results in the numerical simulations. The value of the noise γ_{R} for each condition is also shown. In the three conditions, the estimated interaction parameters lie in the critical region and the three phase diagrams are relatively similar, contrary to what is found for $N = 25$.

values of P and M, but their relative position with respect to the transition region between phases, i.e., the location of the white cross with respect to where the contour lines are more tightly packed. In the polarization diagram [Fig. 5(a)], the system is in the dark-red region, well below the transition line, and in the milling diagram [Fig. 5(g)], the system is almost at the top region in light blue. This situation corresponds to a nonstressed state, almost identical to the one observed in the Control condition [Figs. 5(c) and 5(i), $P < 0.2, M = 0.9$], which represents the system's relaxed state when no external stress is applied.

When the light is switched on (i.e., in the Light period of the Stressing condition), the system jumps into the transition region, where small changes in the parameters induce significant changes in P and M. Comparing the three figures for each light condition and in both measures P [Figs. 5(a)–5(c)] and M [Figs. 5(g)–5(i)], the white cross clearly shifts from the interior of a phase into the transition region. In the diagrams of fluctuations [Figs. 5(d)–5(f) and Fig. 5(j)–5(l)], the white cross is located in the region of small values in the Dark and Control conditions, while in a region of higher values in the Light condition (not in the region of highest fluctuations, due to the limited size of the system).

This scenario corresponds to what one would expect from a biological perspective. Initially, the fish are in a nonstressed resting state. When the stressing stimulus is applied, they move to a critical state in which they can quickly adjust their behavior. Then, after the stimulus, they progressively relax, eventually returning to the Control state.

When a system is close to a transition region, the relaxation times tend to be longer (ultimately diverging in very large systems). Despite the small size of our system, this behavior is suggested by the results of Figs. 2(d)–2(f). When suddenly changing from the Dark to the Light period in the Stressing condition, all three measures, polarization, milling, and dispersion, abruptly shift to new values, and then slowly relax towards the values of the Control condition. This gradual relaxation is particularly noticeable in the dispersion shown in Fig. 2(f). Here the relaxation interval is too short to reach the stationary state. In turn, when the system moves back from Light to Dark, the relaxation time is much shorter, as expected when far from a transition region. We estimated these relaxation times (see Fig. S2 [34]), showing that the relaxation from the critical state in Light is approximately one order of magnitude longer than when returning to Dark ($\tau = 95.3$ s vs $\tau = 12.7$ s), thus suggesting that, in the Light condition, the system relaxes more slowly, which would be consistent with being close to a critical state.

For $N = 25$, the situation is thus as follows: the fish are initially calm, then when a stress stimulus occurs, they quickly shift closer to the transition region to be able to quickly react to potential danger. If nothing happens, they gradually relax, slowly returning to their steady state.

The situation is different for $N = 10$. Figure 6 shows that the changes in polarization and milling are smaller than in the larger group. In fact, the three phase diagrams, corresponding to each light condition, are nearly identical in terms of both P [Figs. 6(a)–6(c)] and M [Figs. 6(g)–6(i)]. In addition, the fluctuation diagrams for the Dark and Light periods in the Stressing condition are also similar [Figs. 6(d), 6(e), 6(j), 6(k)]. Although a slight increase in P is observed in the Light period, the interaction parameters (white cross) remain essentially in the same place, inside the transition region. Thus, in the three phase diagrams, the parameters corresponding to the experiment are located in the transition regions for the polarization and milling order parameters. In fact, since the parameters for the Dark and Control conditions are already in the transition region, it is not surprising to also find that the parameters for the stressed Light condition lie in the same regions. This suggests that in such small groups, the fish are already experiencing a stress state in both the Dark period and the Control condition, and that switching on the light induces only a small additional stress. One possible explanation is that groups of only 10 individuals experience an inherently stressful condition because the typical group size for this fish species in nature is around 30 individuals. It could also be that, since a group of 10 has a higher proportion of individuals near the periphery compared to a group of 25, a certain level of anxiety may persist. A social buffering effect, where the presence of others reduces stress levels in social species, could explain why smaller groups experience more stress [23,24,36–38]. Thus, the reduced behavioral changes across the different light conditions (all in the transition regimes) may reflect a state of constant vigilance rather than a true transition in the response to an additional stress.

III. DISCUSSION

Identifying the mechanisms by which animal groups change their collective state is a key step to understanding how these systems adapt to environmental conditions [39]. In this work we have investigated the mechanisms by which fish schools tune their collective state in response to controlled mild stress. Previous works have found signatures of critical state in fish schools through the analysis of spontaneous behavioral cascades, where large turns in the direction of motion of individuals propagate across a group [19,20]. The power-law distributions of cascade duration, size, and interevent times have provided evidence of scale-free behavior in schooling fish, suggesting that these systems were operating near a phase transition between two collective states. In this region of the parameter space, the school exhibits multistability and regularly shifts between the two states, its responsiveness to perturbations is maximum, and information can quickly propagate across arbitrarily large scales [9–11]. Other works have pointed out that fish schools can also regulate the distance to criticality according to the risk and noise of the environment [21].

Here we used a data-driven computational modeling approach to quantify where in the parameter space groups of rummy-nose tetras operate both in an unperturbed condition and when all fish experience stress. We also studied the impact of group size on individual and collective behavior. In each condition, we measured the polarization, milling, and cohesion of the group. We then used the burst-and-coast model introduced in [25,26,31] to account for collective swimming and light-induced modulation of social interactions [33] in *H. rhodostomus* to determine the values of noise (γ_R), attraction (γ_{Att}), and alignment (γ_{Ali}) parameters that lead to the experimentally measured values of polarization, milling, and

cohesion under these conditions. This procedure allowed us to locate the actual observed fish collective state in the model phase diagram, and to assess the possible proximity of this state to the critical lines estimated from the maxima of the fluctuations of the polarization and milling order parameters.

Our experimental and simulation results indicate that the collective state of fish and their reaction to a stressing condition depend on the size of the group to which they belong. In the Control condition and also in the Dark period of the Stressing condition, while groups of 25 fish are clearly in the milling phase (i.e., far from a critical region), groups of 10 fish are located in the transition region for the polarization and milling order parameters suggesting that individuals are experiencing a stress state presumably because they usually swim in larger groups in the wild [40] or in the fish facility. These results suggest that group size, presumably through a social buffering effect, modulates the strength of interactions between fish and their level of stress [23,36,37]. Empirical studies have shown that the presence of peers is effective in reducing an individual's cortisol or corticosterone response to stress [24,38], thus making individuals living in groups more relaxed/less stressed than when they are alone. A similar group size effect has been demonstrated in other species such as *Kuhlia mugil* in which an increase in fish density within a tank leads to a decrease in the strength of social interactions [41].

Moreover, when the transition between the Dark and the Light period of the Stressing condition occurs, in groups of 10 fish individuals react by increasing their randomness (i.e., increasing the amplitude of the spontaneous heading change) and their tendency to move closer to their peers, while in groups of 25 fish, individuals decrease their randomness and strengthen their tendency to stay aligned with their peers. However, while groups of 10 fish remain inside the transition region between the two phases of schooling and milling, groups of 25 fish move from the milling phase into the transition region when light is switched on. It is precisely in this zone of the parameter space that the fluctuations of the schooling and milling parameters are the largest [Figs. 5(d)–5(f) and Figs. 5(j)–5(l)], and where the sensitivity and reactivity of the shoal are maximal [9–11]. Altogether, these results suggest that when fish are stressed, they readily tune the strength of their social interactions so that the group collectively reaches a critical state which allows a fast adaptation of its behavior in response to changes occurring in the environment. However, as the level of stress of fish is itself modulated by the size of the group, a small group of 10 individuals will immediately operate in a critical state while an additional level of stress induced by the sudden change of illumination is needed to lead a larger group of 25 fish in the critical regime. Furthermore, a large group will allow individuals to quickly return to a relaxed state, whereas in small groups, fish are in a relatively higher level of stress, which will maintain the group in a critical state.

In groups of 25 fish, the transition toward criticality observed under stress corresponds primarily to a polarization transition rather than a milling transition. This is biologically consistent with the idea that increased alignment and cohesion under perceived threat allow the school to rapidly adopt an escape trajectory, a phenomenon observed in other species such as three-spined sticklebacks and golden shiners [42,43]. By contrast, we did not observe a comparable transition toward milling, which suggests that in rummy-nose tetras, vortex-like configurations are not favored under sudden perturbations.

Our data-driven burst-and-coast model accurately reproduces not only qualitatively but also quantitatively the state transition of fish under stress in the two group sizes, including the temporal changes and probability density distributions of several fine observables used to characterize the collective state of the fish.

Some studies have suggested that one possible mechanism used by fish to regulate their collective state under perceived risk involves changes in the structure of the interaction network between individuals [43]. In our work, using a model in which each fish interacts only with its two most influential neighbors, we found that changes in perceived risk and group size modulate the intensity of social interactions. Within the constraints of our model, the interaction network structure implicitly emerges from the notion of the most influential neighbors, and only the interaction strengths are explicitly varied. This suggests that modulation of interaction strength can be sufficient to regulate collective behavior under varying environmental conditions. However, in real biological systems, adjustments in the number of effective neighbors could also occur. From a cognitive perspective, regulating interaction strength rather than network structure may offer a simpler mechanism, as it could maintain a constant cognitive load on individuals [26,44].

In conclusion, this work made it possible to reveal and model the mechanisms underlying collective state transition phenomena observed in fish [27,45,46] and the conditions under which these animal groups can reach a critical state.

IV. MATERIALS AND METHODS

A. Experiments and data collection

1. Ethics statement

Experiments were approved by the local ethical committee for experimental animals and were performed in an approved fish facility (A3155501) under permit APAFIS no. 27303-2020090219529069 v8 in agreement with French legislation.

2. Study species

Rummy-nose tetras (*Hemigrammus rhodostomus*) were purchased from Amazonie Labège in Toulouse, France. This is a small freshwater fish that forms highly cohesive and polarized schools [47,48]. Fish were kept in 16 liter aquariums on a 12:12 hour, dark:light photoperiod, at 24.9 °C (±0.8 °C) and were fed *ad libitum* with fish flakes. The average body length (BL) of the fish used in these experiments is 3.1 cm.

3. Experimental setup

We used a rectangular glass tank of 120 cm × 120 cm supported by a structure of metal beams 20 cm high, inside which was installed a circular white arena of radius $R = 25$ cm. The tank was filled with 7 cm of water of controlled quality (50% of water purified by reverse osmosis and 50% of water treated by activated carbon) heated at 27.11 °C (±0.54 °C). The tank was surrounded by white opaque curtains, and

the experimental room was lit by portable remote-controlled LED lights, ensuring uniform lighting. The illumination of the circular arena was remotely controlled to produce either a constant level of light (25 lx) or an intermittent lighting (0.5 lx, 25 lx). Fish movements were recorded with a high-resolution monochrome camera (Basler acA4024-29uc) from above the setup at 30 Hz (1500 × 1500 p) in the control experiments and at 25 Hz (1920 × 1080 p) in the intermittent light experiments.

4. Experimental design

For each group size $N = 10$ and 25 fish, we carried out a total of 10 experiments that included four replicates in the *Control* condition, where light intensity was kept constant at 25 lx for 1 h, and six replicates in the *Stressing* condition, in which light intensity alternates over 10 periods of 3 min consisting of 2 min at low light intensity (0.5 lx) followed by 1 min at a high light intensity (25 lx). The transition between light intensities was instantaneous and remotely controlled (see Fig. 1). The duration of the low light intensity time interval was chosen so that fish can quickly recover from the Stressing condition and adopt their default state when they are in the dark. The duration of the high light intensity interval was chosen so that fish had time to react to the change in brightness and adapt their behavior to cope with the Stressing condition. The number of periods in the stress conditions was large enough to allow the acquisition of experimental data within a reasonable time, and small enough to avoid possible conditioning or habituation effects to intermittent lighting; see the boxplots in Fig. S1 [34].

Before each session, fish were introduced in the experimental tank with an acclimation of 10 min at 25 lx in the Control condition and at 0.5 lx in the Stressing condition. In all experimental runs performed on the same day, we used different fish, and the intermittent light experiments were spaced out by 1 week to prevent conditioning or habituation phenomena.

5. Data extraction and preprocessing

Raw data thus represent a total of 14 h of video. We then used FastTrack [49] to extract fish trajectories from the videos (i.e., the 2D position of each fish at each frame). Due to the frequent cross-occlusion between individuals and the misidentification of individuals in low light conditions, the tracking accuracy (i.e., the percentage of frames in which all N fish have been correctly identified) varies between 90% and 99% in the Control condition, and 51% and 91% in the Stressing condition (see Table S1 [34] for details on tracking accuracy and [33] in which the same tracking procedures were used).

B. Quantification of collective behavior

We characterize the collective behavioral patterns exhibited by fish groups by means of three observables.

We first define $\vec{u}_i = (x_i, y_i)$ and $\vec{v}_i = (v_x^i, v_y^i)$ as the position and velocity vectors of fish i [see Fig. 7(a)], and $\vec{u}_B = (x_B, y_B)$ and $\vec{v}_B = (v_x^B, v_y^B)$ as the position and velocity vectors of the

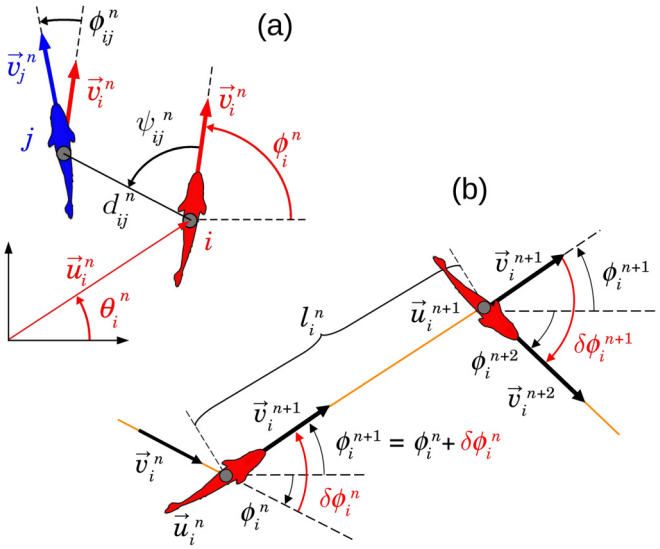

FIG. 7. Variables used to describe social interactions between fish and their burst-and-coast swimming mode. (a) Individual (red) and social (black) state variables of fish i with respect to fish j at the instant t_i^n when fish i performs its nth kick: $\vec{u}_i^n$ and $\vec{v}_i^n$ are the position and velocity vectors of fish i, θ_i^n and ϕ_i^n are the angles that these vectors make with the horizontal line, $\vec{v}_j^n$ is the velocity vector of fish j at time t_i^n, d_{ij}^n is the distance between fish i and fish j, ψ_{ij}^n is the angle with which fish j is perceived by fish i (not necessarily equal to ψ_{ji}^n), and $\phi_{ij}^n = \phi_j^n - \phi_i^n$ is the heading difference between both fish. (b) Schematic of the nth kick performed by fish i moving from $\vec{u}_i^n$ at time t_i^n to $\vec{u}_i^{n+1}$ at time t_i^{n+1} along a distance l_i^n. Orange lines denote fish trajectory, black wide arrows denote velocity vector, curved arrows represent angles. The heading angle change of fish i at time t_i^n is $\delta\phi_i^n$. Fish heading during its nth kick is $\phi_i^{n+1} = \phi_i^n + \delta\phi_i^n$. Red angles show the heading variation of the fish at the kicking instants t_i^n and t_i^{n+1}.

barycenter B of the group, where

$$x_B = \frac{1}{N}\sum_{i=1}^{N} x_i, \quad v_x^B = \frac{1}{N}\sum_{i=1}^{N} v_x^i,$$

with similar expressions for y_B and v_y^B. We assume that the heading angle of fish i is given by its velocity vector, $\phi = \texttt{ATAN2}(v_y, v_x)$. Similarly, the heading angle the barycenter of the group is given by $\phi_B = \texttt{ATAN2}(v_y^B, v_x^B)$.

The three dimensionless observables used to quantify the group behavior at instant t are defined as follows:

(1) Polarization order parameter, $P(t) \in [0, 1]$:

$$P(t) = \frac{1}{N}\left\| \sum_{i=1}^{N} \vec{e}_i(t) \right\|, \tag{1}$$

where $\vec{e}_i = \vec{v}_i / \|\vec{v}_i\|$ is the unit vector in the direction of motion of fish i. Values of $P(t)$ close to 1 mean that N fish are aligned and move in the same direction. Values of P close to 0 indicate that the N vectors point in different directions, but can also mean that vectors are collinear and in opposite directions so that they cancel each other (e.g., when half of the vectors pointing north and the other half pointing south, like when fish are milling). Configurations in which fish are randomly

aligned give rise to values of P of order $1/\sqrt{N}$ ($\langle P\rangle = \frac{1}{2}\sqrt{\frac{\pi}{N}}$ and $\sqrt{\langle P^2\rangle} = \frac{1}{\sqrt{N}}$ for truly uncorrelated headings).

(2) Milling order parameter, $M(t) \in [0, 1]$:

$$M(t) = \frac{1}{N}\left|\sum_{i=1}^{N} \sin\left(\bar{\theta}_{\rm w}^{i}(t)\right)\right|, \tag{2}$$

where $\bar{\theta}_{\rm w}^{i}(t) = \bar{\phi}_i(t) - \bar{\theta}_i(t)$. Variables with a bar are defined in the barycenter system of reference: $\bar{x}_i = x_i - x_{\rm B}$, $\bar{v}_x^i = v_x^i - v_x^{\rm B}$ and similar expressions are used for the y components. The relative position and heading angles of fish i with respect to B are, respectively, $\bar{\theta}_i = \texttt{ATAN2}(\bar{y}_i, \bar{x}_i)$ and $\bar{\phi}_i = \texttt{ATAN2}(\bar{v}_y^i, \bar{v}_x^i)$. The milling order parameter $M(t)$ is similar to an angular momentum and quantifies how much the fish turn in the same direction around the center of the tank, independently of the direction of rotation.

(3) Dispersion $D(t)$:

$$D(t) = \frac{1}{R}\sqrt{\frac{1}{N}\sum_{i=1}^{N} \|\vec{u}_i(t) - \vec{u}_{\rm B}(t)\|^2}, \tag{3}$$

where R is the radius of the fish tank. Large values of $D(t)$ mean that fish are dispersed in the tank, while small values mean that they are aggregated. Note that the dispersion, characterizing the spatial extent of the group, is *not* an order parameter, but it provides valuable complementary information about the collective state of the group.

In order to estimate the sensitivity of fish to light stimuli, we measure the variance of these observables over a period of time, times the group size,

$$\mathcal{X}_A = N \times (\langle A^2(t)\rangle - \langle A(t)\rangle^2), \tag{4}$$

where symbol $\langle\cdot\rangle$ means average over time and A can be the dispersion D, the polarization P, or the milling M.

We also used two additional observables, the distance of each fish to the wall $r_{\rm w}^i = R - |\vec{u}_i|$, where R is the radius of the tank, and the distance of fish to the nearest neighbor NND. Figures 8 and 9 show, respectively, the time series and PDF of these observables.

C. Computational model

We use the burst-and-coast model introduced in [25] and [26,31] to account for collective swimming behavior in *H. rhodostomus* and extended in [33] to account for the impact of varying levels of light intensity on social interactions between fish.

As found in [33], the model can remarkably reproduce the experimental results of fish swimming under different light intensities (0.5, 1, 1.5, 5, and 50 lx) for a wide range of group sizes ($N = 1$, 2, 5, and 25). Both the structure of the model and the shape of the interaction functions (i.e., their analytical expressions) are preserved here, the simple adjustment of the strength and range parameters of the interactions being sufficient to reach an excellent agreement between the numerical simulations and the experimental results.

The model, reflecting the burst-and-coast swimming mode of rummy-nose tetra, considers that fish trajectories are made of a succession of segments, along which fish keep their orientation while decelerating due to the water drag. The short

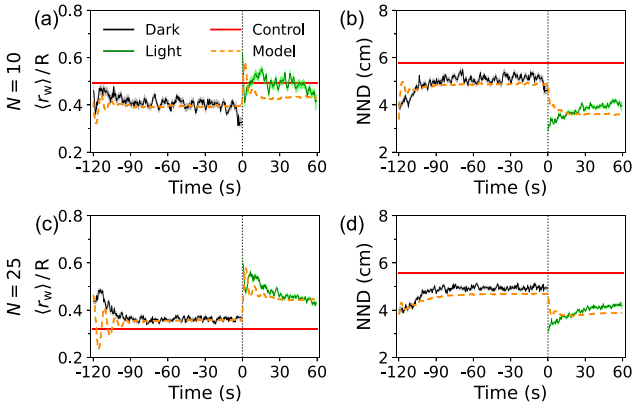

FIG. 8. Time series of the average distance of fish to the wall $\langle r_{\rm w}\rangle/R$ and the average distance of fish to the nearest neighbor (NND) in the experiments. (a), (b) $N = 10$ fish and (c), (d) $N = 25$ fish in the Dark (black lines) and Light (green lines) periods of the Stressing condition and in the Control condition (red lines). Shadows represent the 68% confidence interval (bootstrap of 1000 rounds) for experimental results. Orange dashed lines represent the model simulations.

events between segments (of typical duration 0.1 sec for real fish; considered as instantaneous in the model) during which a fish changes both its velocity and also its direction of motion are called "kicks." The individual state of a fish i at the instant t_i^n when it performs its nth kick is determined by its position and its heading angle, $\vec{u}_i^n$ and ϕ_i^n, respectively. Precisely at time t_i^n, the fish chooses its new heading $\phi_i^{n+1} = \phi_i^n + \delta\phi_i^n$, where $\delta\phi_i^n$ is the heading angle change, and glides along a straight line of length l_i^n, with an initial speed v_i^n, and during a time τ_i^n.

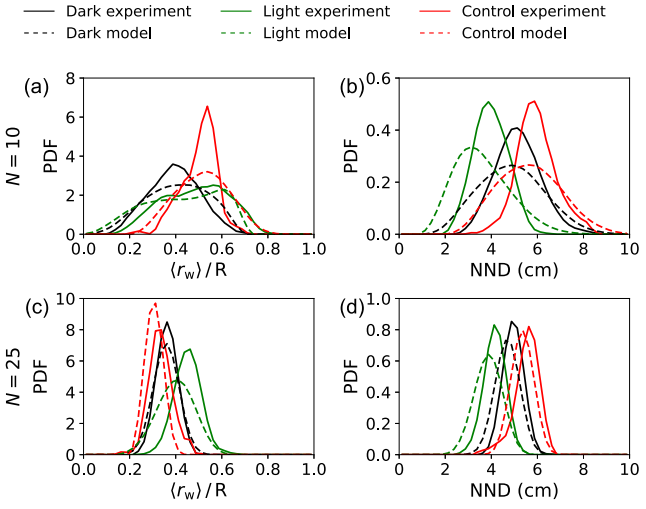

FIG. 9. Probability density functions (PDF) of the distance to the wall $\langle r_{\rm w}\rangle/R$ and the distance to the nearest neighbor (NND) observed in the experiments (solid lines) and obtained in the numerical simulations (dashed lines). (a), (b) $N = 10$ fish and (c), (d) $N = 25$ fish in the Dark (black lines) and Light (green lines) periods of the Stressing condition and in the Control condition (red lines).

At the end of the kick, at time $t_i^{n+1} = t_i^n + \tau_i^n$, the new position and heading are given by

$$\phi_i^{n+1} = \phi_i^n + \delta\phi_i^n, \tag{5}$$

$$\vec{u}_i^{n+1} = \vec{u}_i^n + l_i^n\,\vec{e}\left(\phi_i^{n+1}\right), \tag{6}$$

where $\vec{e}(\phi_i^{n+1})$ is the unit vector of the direction of motion of the fish during its nth kick, given by ϕ_i^{n+1} [see Fig. 7(b)].

In this model, the length, initial speed, and duration of the kicks performed by a fish are independent of those performed by other fish. The duration and speed are sampled from bell-shaped distributions resembling the experimental ones, and given by

$$\tau_i^n = \tau_{\text{avg}}\sqrt{-4\log\left(\xi_i^n\right)/\pi}, \quad v_i^n = v_{\text{avg}}\sqrt{-4\log\left(\eta_i^n\right)/\pi},$$

where τ_{avg} and l_{avg} are the average kick duration and length measured in the experiments, and ξ_i^n and η_i^n are two random numbers uniformly distributed in (0,1). Assuming an exponential decay of the speed between kicks (fully consistent with experiment [25]), the peak speed v_i^n and the kick duration and length τ_i^n and l_i^n are linked by the relation, $l = v\tau_0[1 - \exp(-\tau/\tau_0)]$, where τ_0 is a decay time. Then the position of fish i at any intermediate time $t_i^n + \Delta t$ in $[t_i^n, t_i^{n+1}]$ can be calculated as follows:

$$\vec{u}\left(t_i^n + \Delta t\right) = \vec{u}_i^n + l_i^n \frac{1 - \exp(-\Delta t/\tau_0)}{1 - \exp\left(-\tau_i^n/\tau_0\right)}\,\vec{e}\left(\phi_i^{n+1}\right), \tag{7}$$

where $0 \leqslant \Delta t \leqslant \tau_i^n$.

The heading angle change of an individual fish $\delta\phi$ results from the additive combination of its spontaneous behavior, the physical constraints of the environment (e.g., obstacles), and the social interactions with other fish:

$$\delta\phi = \delta\phi^{\text{R}} + \delta\phi^{\text{W}} + \delta\phi^{\text{S}}, \tag{8}$$

where indices R, W, and S stand for Random, Wall, and Social, respectively. The analytical expressions of these forces were derived in [25] for pairwise interactions by means of a procedure of reconstruction applied to experimental data of pairs of fish. Here we use a simplified version introduced in [26] for groups of larger size.

The spontaneous heading change of fish can be described by a Gaussian noise when the fish swims alone far from the wall, and their amplitude is smaller when the fish comes close to the wall. Thus,

$$\delta\phi^{\text{R}} = \gamma_{\text{R}}\left(1 - \alpha\exp\left[-\left(\frac{r_{\text{w}}}{l_{\text{w}}}\right)^2\right]\right)g, \tag{9}$$

where γ_{R} is the amplitude of these heading changes, l_{w} is the distance of fish to the wall from which the amplitude is reduced, α is the strength of this reduction, and g is a Gaussian random variable with zero average and unit variance.

The wall exerts on the fish a repulsive force that depends only on the distance of the fish to the wall r_{w} and its relative orientation to the wall θ_{w}. We assume that this dependence is decoupled, so that the heading angle change due to this force can be written as

$$\delta\phi^{\text{W}}(r_{\text{w}}, \theta_{\text{w}}) = f_{\text{w}}(r_{\text{w}})O_{\text{w}}(\theta_{\text{w}}), \tag{10}$$

$$f_{\text{w}}(r_{\text{w}}) = \gamma_{\text{w}}\exp[-(r_{\text{w}}/l_{\text{w}})^2], \tag{11}$$

$$O_{\text{w}}(\theta_{\text{w}}) = \beta_{\text{w}}\sin(\theta_{\text{w}})[1 + 0.8\cos(2\theta_{\text{w}})], \tag{12}$$

where γ_{w} is the intensity and l_{w} the range of the wall repulsion, and β_{w} is a constant of normalization of the angular function so that the mean of the squared function in $[-\pi, \pi]$ is equal to 1: $\frac{1}{2\pi}\int_{-\pi}^{\pi} O_{\text{w}}^2(\theta)\,d\theta = 1$.

The social interactions between fish i are considered to be the linear combination of pairwise interactions $\delta\phi_{ij}^{\text{S}}$ with a specific number of neighbors $j = 1, \ldots, k$. The pairwise interactions $\delta\phi_{ij}^{\text{S}}$ depend only on the relative state $s_{ij} = (d_{ij}, \psi_{ij}, \phi_{ij})$ of fish j with respect to fish i, given by the distance between them d_{ij}, the viewing angle ψ_{ij} with which fish i perceives fish j, and their relative alignment $\phi_{ij} = \phi_j - \phi_i$. It has been shown in [25,26] that in *H. rhodostomus*, each fish interacts with its neighbors by means of an attraction interaction (negative/repulsive at short range) and an alignment interaction, and selectively interacts with the $k = 2$ specific neighbors having the largest and the second-largest associated value of $|\delta\phi_{ij}^{\text{S}}|$. Thus,

$$\delta\phi_i^{\text{S}}(s_{ij}) = \delta\phi_{i1}^{\text{S}}(s_{ij}) + \delta\phi_{i2}^{\text{S}}(s_{ij}), \tag{13}$$

$$\text{where} \quad \delta\phi_{ij}^{\text{S}}(s_{ij}) = F_{\text{Att}}(s_{ij}) + F_{\text{Ali}}(s_{ij}), \tag{14}$$

$$\text{and} \quad F_{\text{Att}}(s_{ij}) = f_{\text{Att}}(d_{ij})\,O_{\text{Att}}(\psi_{ij})\,E_{\text{Att}}(\phi_{ij}), \tag{15}$$

$$F_{\text{Ali}}(s_{ij}) = f_{\text{Ali}}(d_{ij})\,O_{\text{Ali}}(\phi_{ij})\,E_{\text{Ali}}(\psi_{ij}), \tag{16}$$

for $j = 1, 2$. The analytical expressions found for these functions were extracted from specific experiments under different uniform light intensities and are as follows [33]:

$$f_{\text{Att}}(d) = \gamma_{\text{Att}}\frac{d/d_{\text{Att}} - 1}{1 + (d/l_{\text{Att}})^2}, \tag{17}$$

$$O_{\text{Att}}(\psi) = \beta_{\text{Att}}\sin(\psi)[1 - 0.33\cos(\psi)], \tag{18}$$

$$E_{\text{Att}}(\phi) = \lambda_{\text{Att}}[1 - 0.6\cos(\phi) - 0.4\cos(2\phi)], \tag{19}$$

for the attraction, and, for the alignment:

$$f_{\text{Ali}}(d) = \gamma_{\text{Ali}}\frac{d}{d_{\text{Ali}}}\exp\left[-\left(\frac{d}{l_{\text{Ali}}}\right)^2\right], \tag{20}$$

$$O_{\text{Ali}}(\phi) = \lambda_{\text{Ali}}\sin(\phi)[1 + 0.33\cos(\phi)], \tag{21}$$

$$E_{\text{Ali}}(\psi) = \beta_{\text{Ali}}[1 + 1.18\cos(\psi) - 0.49\cos(2\psi)]. \tag{22}$$

Here γ_{Att} and γ_{Ali} are the dimensionless intensities of the attraction and alignment forces, respectively, d_{Att} and d_{Ali} are the distance below which the corresponding interaction changes sign, l_{Att} and l_{Ali} are the respective ranges of action, and β_{Att}, λ_{Att}, β_{Ali}, and λ_{Ali} are the constants of normalization of the corresponding angular function. The parameter values are given in Table II and Fig. 10.

Finally, a rejection procedure is used when the position of the fish calculated at the end of the kick is out of the tank. In that case, the kick is rejected, a new kick is calculated, a new angle of spontaneous variation $\delta\phi^{\text{R}}$, a new kick length l_i^n and

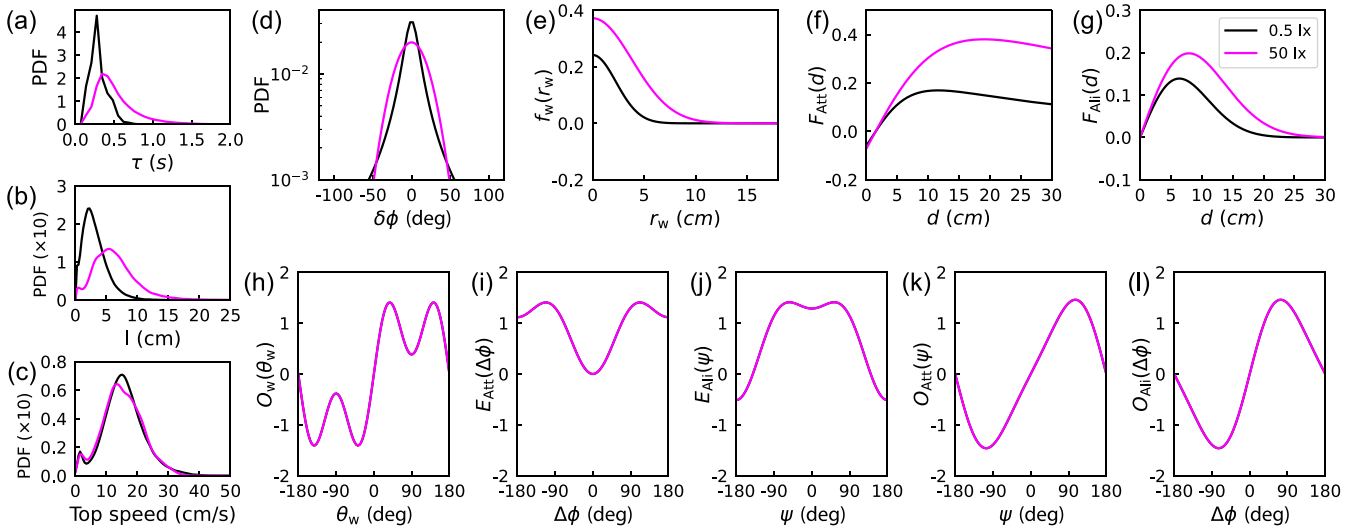

FIG. 10. Functions used in the model to account for the effects of light intensity on the burst-and-coast swimming and the social interactions between pairs of fish derived from [33]. Probability density function (PDF) of (a) the kick duration τ, (b) the kick length l, (c) the peak speed at the kicking instant v, and (d) the spontaneous heading change $\delta\phi$. (e) Repulsion from the wall $f_w(r_w)$ as a function of the distance to the wall r_w. (f), (g) Attraction $F_{Att}(d)$ and alignment $F_{Ali}(d)$ as function of the distance between fish d. (h) Repulsion from the wall $O_w(\theta_w)$ as a function of the relative orientation of the fish to the wall θ_w, (i), (j) Attraction between fish $E_{Att}(\Delta\phi)$ and $O_{Att}(\psi)$ as a function of the relative orientation between fish $\Delta\phi$ and the viewing angle ψ respectively, (k), (l) Alignment between fish $O_{Ali}(\psi)$ and $E_{Att}(\Delta\phi)$ as functions of the viewing angle ψ and as a function of the relative orientation between fish $\Delta\phi$. O and E indicate the parity of the function, odd and even, respectively. Black lines correspond to 0.5 lx, pink lines to 50 lx.

a new kick duration τ_i^n are sampled, until the final position at the end of the kick is inside the tank. If no suitable kick is found after 1000 tries, $\delta\phi^R$ is randomly sampled from a uniform distribution (see [25] for more details).

D. Numerical simulations and parameters estimation from experiments

Three series of numerical simulations of the burst-and-coast model were carried out. The first one was performed to get accurate values of the parameters $(\gamma_R, \gamma_{Att}, \gamma_{Ali})$ for each condition: the Control condition (25 lx), the Dark period of the Stressing condition (0.5 lx), and the Light period of the Stressing condition (25 lx). In the second series of simulations, we run the model under each experimental condition, and the third series was performed to build the corresponding phase diagrams.

TABLE II. Model parameters used in the simulations of different illumination conditions and different group sizes.

	$N = 10$			$N = 25$		
Parameter	Dark	Light	Ctrl	Dark	Light	Ctrl
γ_w	0.3	0.4	0.4	0.3	0.4	0.4
β_w			1.9612			
l_w (m)	0.031	0.053	0.053	0.031	0.053	0.053
α	0.35	0.66	0.66	0.35	0.66	0.66
d_{Att} (m)			0.015			
β_{Att}			1.43			
λ_{Att}			0.9			
l_{Att} (m)	0.1	0.165	0.165	0.1	0.165	0.165
d_{Ali} (m)			0.015			
β_{Ali}			0.9			
λ_{Ali}			1.43			
l_{Ali} (m)	0.092	0.135	0.135	0.092	0.135	0.135
τ_{avg} (s)	0.32	0.55	0.55	0.32	0.55	0.55
τ_0 (s)	0.34	0.86	0.86	0.34	0.86	0.86
l_{avg} (m)	0.028	0.053	0.053	0.028	0.053	0.053

1. Parameter values

The parameter values used in the model are those determined in [33] for different light intensities and group sizes. Parameter values corresponding to the light intensity of 25 lx were obtained by interpolation from measurements made at 5 lx and 50 lx by [33]. Likewise, the parameter values for the groups of $N = 10$ were obtained by interpolation from measurements done in groups of five and 25 fish at different light intensities in [33]. Note, however, that in [33] the parameter values were measured with a constant illumination. Therefore, we have to take into account the modulation of individual parameters caused by sudden changes in light intensity. According to the results reported in [31], the amplitude of individuals' spontaneous heading change, γ_R, as well as the strength of social interactions between fish, γ_{Att} and γ_{Ali}, can deeply affect the group behavior. Therefore, we assume that intermittent illumination causes changes in $\boldsymbol{\gamma} = (\gamma_R, \gamma_{Att}, \gamma_{Ali})$ without affecting other parameters. The estimation procedure to find out their values is given below.

We used the mean values and the PDFs of the three observables P, M, and D to quantify the agreement between the numerical simulations of the model and the experimental results. For each light condition and group size, we

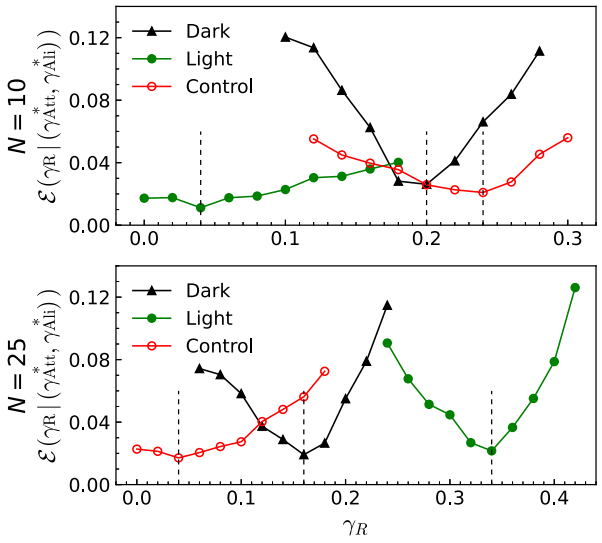

FIG. 11. Determination of $\gamma^* = (\gamma_R^*, \gamma_{Att}^*, \gamma_{Ali}^*)$, the triplet that minimizes the total error function $\mathcal{E}$ defined in Eq. (23) as a function of γ_R, for each condition and each group size. γ_{Att} and γ_{Att} have been optimized for each value of γ_R for $N = 10$ (top) and $N = 25$ (bottom) in the Dark (black lines) and Light (green lines) periods of the Stressing condition and in the Control condition (red lines). The vertical dotted lines indicate the value of γ_R that minimizes the error function.

run a large number of numerical simulations to find the triplet $\boldsymbol{\gamma}^* = (\gamma_R^*, \gamma_{Att}^*, \gamma_{Ali}^*)$ that minimizes the total error given by

$$\mathcal{E}(\boldsymbol{\gamma}) = |D_{sim}(\boldsymbol{\gamma}) - D_{exp}| + |P_{sim}(\boldsymbol{\gamma}) - P_{exp}| + |M_{sim}(\boldsymbol{\gamma}) - M_{exp}|. \quad (23)$$

This is done in two steps. First, for each fixed value of γ_R, we sweep through the plane γ_{Att}-γ_{Ali} with a fine discretization and find the pair $(\gamma_{Att}, \gamma_{Ali})$ that yields the smallest error $\mathcal{E}(\gamma_R)$.

Figure 11 shows the resulting curves $\mathcal{E}(\gamma_R)$ for each group size and each light condition. Then we sweep through the values of γ_R and the corresponding pairs $(\gamma_{Att}, \gamma_{Ali})$ obtained for each one and find the value of γ_R that yields the smallest error $\mathcal{E}(\boldsymbol{\gamma}^*)$. These values are represented by vertical dashed lines in Fig. 11, for each condition and each group size. We used a discretization of 10 values of γ_R with a step of 0.02 in different subintervals of $[0, 0.42]$, depending on the group size and the condition, and a fine step $\Delta\gamma = 10^{-3}$ to sweep the γ_{Att}-γ_{Ali} plane. The final parameter values are given in Table II.

The simulations carried out to find the value $\boldsymbol{\gamma}^*$ in the Control condition were performed in the same conditions as the experimental ones. We simulated 10 runs of 70 min at 25 lx, the first 10 min of each run corresponding to the habituation time. We only used the last 60 min to calculate the mean values D_{sim}, P_{sim}, and M_{sim}.

For the Stressing condition, numerical simulations were simplified with respect to what is done experimentally. Instead of simulating runs of 10 successive 3-min periods of 2 min in the Dark condition and 1 min in the Light condition, as in the experiments, we proceeded in two steps, first for the Dark condition, then for the Light condition. For the Dark condition, we simulated 600 simple runs of 2 min under constant light. For the Light condition, a jump in light must be considered in the 3-min period which is described below. In both Dark and Light conditions, each run started from an initial condition randomly selected from the initial states obtained in the Dark condition in the experiments. Then the value of $\boldsymbol{\gamma}^*$ minimizing the error is extracted for each Dark and Light condition, using the respective simulated data.

The simulations of the 3-min period in the Light condition were done as follows. According to [33], the three strength parameters γ_R, γ_{Att}, and γ_{Ali} take different values depending on the light intensity. A simple assumption could be made that, when transitioning from Dark to Light, these values jump from those corresponding to the initial light intensity to those corresponding to the new light intensity. Under this assumption, the variation of γ_{Att} and γ_{Ali} could be modeled using piecewise constant functions. However, the simulations of the model using this hypothesis show that the system is not able to adapt quickly enough to the change and remains in the stable state corresponding to the light intensity before the change. We therefore introduce the reasonable assumption that, following an abrupt change in illumination, the fish school undergoes a 30-sec habituation period before reaching a stable behavioral regime. During the Dark period, this implies that γ_{Att} and γ_{Ali} gradually transition over the first 30 sec from the values associated with the preceding Light period to their new stationary values in darkness. Conversely, upon entering the Light period, γ_{Att} and γ_{Ali} exhibit a pronounced initial increase, followed by a smooth decline toward the steady-state values corresponding to the new light intensity. This dynamic allows the fish group to progressively adapt its behavior in response to the evolving values of these parameters (see Fig. 4).

No transition is necessary for γ_R. This mechanism used to account for the transition period was tested by comparing the results of the numerical simulations with the experimental ones. Both the duration of the transition period and the initial value have been determined after successive trials. We tried several decaying rates, and found that a square root behavior provided a smoother transition than a simple linear decay:

$$\gamma_{Att} = \left(\gamma_{Att}^s - \gamma_{Att}^{init}\right)\sqrt{\tau_L/30} + \gamma_{Att}^{init}, \quad (24)$$

$$\gamma_{Ali} = \left(\gamma_{Ali}^s - \gamma_{Ali}^{init}\right)\sqrt{\tau_L/30} + \gamma_{Ali}^{init}, \quad (25)$$

where $\tau_L \in [0, 30]$ is the time elapsed from the beginning of the Dark or Light condition. At $\tau_L = 0$ s, $(\gamma_{Att}, \gamma_{Ali}) = (\gamma_{Att}^{init}, \gamma_{Ali}^{init})$ represent the initial values, and at $\tau_L = 30$ s, $(\gamma_{Att}, \gamma_{Ali}) = (\gamma_{Att}^s, \gamma_{Ali}^s)$ represent the stationary values. In the Dark condition, γ_{Att}^{init} and γ_{Ali}^{init} are reasonably set to the stationary values in Light condition, while in the Light condition, γ_{Att}^{init} and γ_{Ali}^{init} are set to 1.3 and 1.5 times the stable value, respectively.

We run 600 simulations of one period composed of 2 min at 0.5 lx and 1 min at 25 lx, where the first 30 sec of each interval corresponds to the transition from the initial state to the final one (Fig. 4). To calculate the mean values P_{sim}, M_{sim}, and D_{sim}, we used the last 30 sec of each interval of each condition, that is, the last 30 sec of the 600 intervals of 2 min for the Dark

condition, and the last 30 sec of the 600 intervals of 1 min for the Light condition.

2. Simulations of the experimental conditions

Once the values of $\boldsymbol{\gamma}$ have been determined for each group size and illumination condition, a second series of numerical simulations was carried out to reproduce the experiments. These simulations were also used to find the adequate profile of the transition interval.

For the Control condition, we ran 10 simulations of 70 min at 25 lx, the first 10 min being the habituation, and we used the last 60 min to calculate the mean values and the PDFs shown in Figs. 2 and 3. For the Stressing condition, we run 2400 simulations of one period of 3 min including the transition described above. The result is represented by the dashed lines in Figs. 2 and 3. To calculate the corresponding mean values and the PDFs shown in Fig. 3, we used the last 30 sec of each interval of each light condition of the period, that is, the last 30 sec of the 2400 intervals of 2 min for the 0.5 lx light intensity, and the last 30 sec of the 2400 intervals of 1 min for the 25 lx light intensity.

The agreement of the numerical simulations with the experimental results is shown in Figs. 2 and 3, for the three observables of polarization, milling and dispersion, and in Figs. 8 and 9 for the distance to the wall r_w and the distance to the nearest neighbor NND.

3. Construction of the phase spaces

Once the values of γ have been obtained, we built the phase diagrams for each group size for the value of γ_R found with our iterative procedure. Again, mean values of the observables shown in the phase diagrams are obtained by performing 600 simulations of one period for each pair $(\gamma_{Att}, \gamma_{Ali})$, with a discretization step of $\Delta\gamma = 10^{-3}$ in $[0, 0.05] \times [0, 0.05]$, that is, 1.5 million runs for each phase diagram and condition.

ACKNOWLEDGMENTS

This work was partly supported by the Indo-French Centre for the Promotion of Advanced Research (Project No. 64T4-B) to G.T. and V.G. G.L. was supported by the Fundamental Research Funds for the Central Universities (2024XKRC078) and a grant from the China Scholarship Council (CSC No. 202006040162). T.X. was supported by a grant from the China Scholarship Council (CSC No. 202106040094). X.L. was supported by a grant from the China Scholarship Council (CSC No. 202106040093). Z.H. was supported by the National Natural Science Foundation of China (Grant No. 62176022). G.T., R.E., and C.S. were supported by the Agence Nationale de la Recherche (ANR-20-CE45-0006-1).

DATA AVAILABILITY

The data that support the findings of this article are openly available [50], embargo periods may apply.

[1] P. Ball, *The Self-made Tapestry: Pattern Formation in Nature* (Oxford University Press, Oxford, 1999).

[2] M. Moussaid, S. Garnier, G. Theraulaz, and D. Helbing, Collective information processing and pattern formation in swarms, flocks, and crowds, Topics Cognitive Sci. **1**, 469 (2009).

[3] S. Camazine, J.-L. Deneubourg, N. R. Franks, J. Sneyd, G. Theraulaz, and E. Bonabeau, *Self-organization in Biological Systems* (Princeton University Press, Princeton, 2001).

[4] R. Wedlich-Söldner and T. Betz, Self-organization: The fundament of cell biology, Phil. Trans. R. Soc. B **373**, 20170103 (2018).

[5] E. Karsenti, Self-organization in cell biology: A brief history, Nat. Rev. Mol. Cell Biol. **9**, 255 (2008).

[6] C. Wolf and D. E. J. Linden, Biological pathways to adaptability—Interactions between genome, epigenome, nervous system and environment for adaptive behavior, Genes Brain Behav. **11**, 3 (2012).

[7] H. E. Stanley, *Phase Transitions and Critical Phenomena*, International Series of Monographs on Physics Vol. 46 (Clarendon Press, Oxford, 1971).

[8] T. Mora and W. Bialek, Are biological systems poised at criticality? J. Stat. Phys. **144**, 268 (2011).

[9] D. S. Calovi, U. Lopez, P. Schuhmacher, H. Chaté, C. Sire, and G. Theraulaz, Collective response to perturbations in a data-driven fish school model, J. R. Soc. Interface **12**, 20141362 (2015).

[10] M. A. Munoz, Colloquium: Criticality and dynamical scaling in living systems, Rev. Mod. Phys. **90**, 031001 (2018).

[11] P. P. Klamser and P. Romanczuk, Collective predator evasion: Putting the criticality hypothesis to the test, PLoS Comput. Biol. **17**, e1008832 (2021).

[12] J. M. Beggs, The criticality hypothesis: How local cortical networks might optimize information processing, Philos. Trans. R. Soc. A **366**, 329 (2008).

[13] J. M. Beggs and N. Timme, Being critical of criticality in the brain, Front. Physiol. **3**, 163 (2012).

[14] E. Balleza, E. R. Alvarez-Buylla, A. Chaos, S. Kauffman, I. Shmulevich, and M. Aldana, Critical dynamics in genetic regulatory networks: Examples from four kingdoms, PLoS ONE **3**, e2456 (2008).

[15] B. C. Daniels, H. Kim, D. Moore, S. Zhou, H. B. Smith, B. Karas, S. A. Kauffman, and S. I. Walker, Criticality distinguishes the ensemble of biological regulatory networks, Phys. Rev. Lett. **121**, 138102 (2018).

[16] G. De Palo, D. Yi, and R. G. Endres, A critical-like collective state leads to long-range cell communication in dictyostelium discoideum aggregation, PLoS Biol. **15**, e1002602 (2017).

[17] W. Bialek, A. Cavagna, I. Giardina, T. Mora, O. Pohl, E. Silvestri, M. Viale, and A. M. Walczak, Social interactions dominate speed control in poising natural flocks near criticality, Proc. Natl. Acad. Sci. USA **111**, 7212 (2014).

[18] A. Attanasi, A. Cavagna, L. Del Castello, I. Giardina, S. Melillo, L. Parisi, O. Pohl, B. Rossaro, E. Shen, E. Silvestri *et al.*, Finite-size scaling as a way to probe near-criticality in natural swarms, Phys. Rev. Lett. **113**, 238102 (2014).

[19] L. Gómez-Nava, R. T. Lange, P. P. Klamser, J. Lukas, L. Arias-Rodriguez, D. Bierbach, J. Krause, H. Sprekeler, and P. Romanczuk, Fish shoals resemble a stochastic excitable system driven by environmental perturbations, Nat. Phys. **19**, 663 (2023).

[20] A. Puy, E. Gimeno, D. March-Pons, M. C. Miguel, and R. Pastor-Satorras, Signatures of criticality in turning avalanches of schooling fish, Phys. Rev. Res. **6**, 033270 (2024).

[21] W. Poel, B. C. Daniels, M. M. Sosna, C. R. Twomey, S. P. Leblanc, I. D. Couzin, and P. Romanczuk, Subcritical escape waves in schooling fish, Sci. Adv. **8**, eabm6385 (2022).

[22] P. Romanczuk and B. C. Daniels, Phase transitions and criticality in the collective behavior of animals—Self-organization and biological function, in *Order, Disorder and Criticality: Advanced Problems of Phase Transition Theory*, edited by Y. Holovatch (World Scientific, Singapore, 2023), pp. 179–208.

[23] B. M. Culbert, K. M. Gilmour, and S. Balshine, Social buffering of stress in a group-living fish, Proc. R. Soc. B **286**, 20191626 (2019).

[24] K. M. Gilmour and B. Bard, Social buffering of the stress response: Insights from fishes, Biol. Lett. **18**, 20220332 (2022).

[25] D. S. Calovi, A. Litchinko, V. Lecheval, U. Lopez, A. Pérez Escudero, H. Chaté, C. Sire, and G. Theraulaz, Disentangling and modeling interactions in fish with burst-and-coast swimming reveal distinct alignment and attraction behaviors, PLoS Comput. Biol. **14**, e1005933 (2018).

[26] L. Lei, R. Escobedo, C. Sire, and G. Theraulaz, Computational and robotic modeling reveal parsimonious combinations of interactions between individuals in schooling fish, PLoS Comput. Biol. **16**, e1007194 (2020).

[27] K. Tunstrøm, Y. Katz, C. C. Ioannou, C. Huepe, M. J. Lutz, and I. D. Couzin, Collective states, multistability and transitional behavior in schooling fish, PLoS Comput. Biol. **9**, e1002915 (2013).

[28] D. S. Calovi, U. Lopez, S. Ngo, C. Sire, H. Chaté, and G. Theraulaz, Swarming, schooling, milling: Phase diagram of a data-driven fish school model, New J. Phys. **16**, 015026 (2014).

[29] A. Filella, F. Nadal, C. Sire, E. Kanso, and C. Eloy, Model of collective fish behavior with hydrodynamic interactions, Phys. Rev. Lett. **120**, 198101 (2018).

[30] C. Huang, F. Ling, and E. Kanso, Collective phase transitions in confined fish schools, Proc. Natl. Acad. Sci. USA **121**, e2406293121 (2024).

[31] W. Wang, R. Escobedo, S. Sanchez, C. Sire, Z. Han, and G. Theraulaz, The impact of individual perceptual and cognitive factors on collective states in a data-driven fish school model, PLoS Comput. Biol. **18**, e1009437 (2022).

[32] W. Wang, R. Escobedo, S. Sanchez, Z. Han, C. Sire, and G. Theraulaz, Collective phases and long-term dynamics in a fish school model with burst-and-coast swimming, R. Soc. Open Sci. **12**, 240885 (2025).

[33] T. Xue, X. Li, G. Lin, R. Escobedo, Z. Han, X. Chen, C. Sire, and G. Theraulaz, Tuning social interactions' strength drives collective response to light intensity in schooling fish, PLoS Comput. Biol. **19**, e1011636 (2023).

[34] See Supplemental Material at http://link.aps.org/supplemental/10.1103/nr7p-m4ff for three supplementary figures, two supplementary tables, and eight supplementary movies.

[35] C. Aimon, C. Lebigre, S. Le Floch, and G. Claireaux, Effects of dispersant-treated oil upon behavioural and metabolic parameters of the anti-predator response in juvenile european sea bass (*Dicentrarchus labrax*), Sci. Total Environ. **834**, 155430 (2022).

[36] R. M. Ross, T. W. Backman, and K. E. Limburg, Group-size-mediated metabolic rate reduction in American shad, Trans. Am. Fish. Soc. **121**, 385 (1992).

[37] M. B. Hennessy, S. Kaiser, and N. Sachser, DSocial buffering of the stress response: Diversity, mechanisms, and functions, Front. Neuroendocrinol. **30**, 470 (2009).

[38] N. Pagnussat, A. L. Piato, I. C. Schaefer, M. Blank, A. R. Tamborski, L. D. Guerim, C. D. Bonan, M. R. Vianna, and D. R. Lara, One for all and all for one: The importance of shoaling on behavioral and stress responses in zebrafish, Zebrafish **10**, 338 (2013).

[39] M. Galesic, D. Barkoczi, A. M. Berdahl, D. Biro, G. Carbone, I. Giannoccaro, R. L. Goldstone, C. Gonzalez, A. Kandler, A. B. Kao *et al.*, Beyond collective intelligence: Collective adaptation, J. R. Soc. Interface **20**, 20220736 (2023).

[40] R. E. Reis, *Check List of the Freshwater Fishes of South and Central America* (Edipucrs, 2003).

[41] J. Gautrais, F. Ginelli, R. Fournier, S. Blanco, M. Soria, H. Chaté, and G. Theraulaz, Deciphering interactions in moving animal groups, PLoS Comput. Biol. **8**, e1002678 (2012).

[42] N. W. F. Bode, J. J. Faria, D. W. Franks, J. Krause, and A. J. Wood, How perceived threat increases synchronization in collectively moving animal groups, Proc. R. Soc. B **277**, 3065 (2010).

[43] M. M. Sosna, C. R. Twomey, J. Bak-Coleman, W. Poel, B. C. Daniels, P. Romanczuk, and I. D. Couzin, Individual and collective encoding of risk in animal groups, Proc. Natl. Acad. Sci. USA **116**, 20556 (2019).

[44] A. Puy, E. Gimeno, J. Torrents, P. Bartashevich, M. C. Miguel, R. Pastor-Satorras, and P. Romanczuk, Selective social interactions and speed-induced leadership in schooling fish, Proc. Natl. Acad. Sci. USA **121**, e2309733121 (2024).

[45] H. V. Ribeiro, M. R. Acre, J. D. Faulkner, L. R. da Cunha, K. M. Lawson, J. J. Wamboldt, M. K. Brey, C. M. Woodley, and R. D. Calfee, Effects of shady environments on fish collective behavior, Sci. Rep. **12**, 17873 (2022).

[46] B. Lafoux, P. Bernard, B. Thiria, and R. Godoy-Diana, Confinement-driven state transition and bistability in schooling fish, Phys. Rev. E **110**, 034613 (2024).

[47] L. Jiang, L. Giuggioli, A. Perna, R. Escobedo, V. Lecheval, C. Sire, Z. Han, and G. Theraulaz, Identifying influential neighbors in animal flocking, PLoS Comput. Biol. **13**, e1005822 (2017).

[48] V. Lecheval, L. Jiang, P. Tichit, C. Sire, C. K. Hemelrijk, and G. Theraulaz, Social conformity and propagation of information in collective U-turns of fish schools, Proc. R. Soc. B **285**, 20180251 (2018).

[49] B. Gallois and R. Candelier, Fasttrack: An open-source software for tracking varying numbers of deformable objects, PLoS Comput. Biol. **17**, e1008697 (2021).

[50] https://doi.org/10.6084/m9.figshare.29877245.v1.